Research article

Preparation of graft copolymer of chitosan-poly ortho-toluidine for antibacterial properties

Sama Sadat Hosseini [a], Seyed Hossein Hosseini [b,*], Abbas Hajizade [b]

[a] Department of Veterinary, Faculty of Veterinary, Science and Research Branch, Islamic Azad University, Tehran, Iran
[b] Department of Chemistry, Nika Pooyesh Industrial Research Institute, Tehran, Iran

ARTICLE INFO

ABSTRACT

The combination polymers or copolymers have new and combined properties and increase the efficiency of the new polymer. Biopolymers are biodegradable and can play the role of biocompatible and biodegradable in composite polymers. Therefore, poly ortho–toluidine was grafted on chitosan (Cs-*g*-POT) by chemical and electrochemical polymerization methods. Cs-*g*-POT was characterized by FTIR, UV–visible, and ^{1}H NMR spectroscopy techniques. The thermal behaviors of the copolymer were investigated by thermogravimetric analysis (TGA) and differential scanning calorimetry (DSC). The images of the surface of the copolymer obtained from imaging SEM confirm the successful attachment of POT on chitosan and indicate that the graft polymerization has been successfully performed with both methods. The percentage and efficiency of engraftment were carefully measured and reported. The electrical conductivity of Cs-*g*-POT was measured by the four-point method and the conductivity was 9.1×10^{-4} S/cm. The copolymer's antibacterial property was studied on *Escherichia coli*, *Staphylococcus aureus*, and *Pseudomonas aeruginosa* as a common bacterium in skin wounds. These studies were investigated using the disk diffusion and minimum inhibitory concentration (MIC) methods. In all tested concentrations the polymer could inhibit the growth of *E. coli* and *P. aeruginosa* significantly. However, it inhibited the growth of *S. aureus* in concentrations above 1 μg. Bacteria are adsorbed on the surface of the polymer by polar-polar and Van Der Waals interactions, where they undergo cell lysis by dopant and electron transfer, and eventually bacterial cell death. Due to its scaffolding properties, this polymer will have a very good use in tissue and bone repair as well as anti-cancer drugs.

1. Introduction

Chitosan (Cs) and other biopolymers are a natural polymer that has many applications due to their good processing properties, solubility, antibacterial properties, and plants [1,2]. The production of Cs copolymers is also widely developed and has various applications in various fields. Most of these applications have been in industry and medicine [3,4]. Conductive polymers are also intelligent polymers with unique electrical properties that are showing great development in the industry every day and have found many applications [5,6].

One of the ways of chemical modification of chitosan that can create various applications is grafting with targeted compounds or polymers. New compounds create biopolymer properties with very diverse applications. Recently, grafted copolymers of chitosan and

* Corresponding author.
  E-mail address: dr.shhosseini@gmail.com (S.H. Hosseini).

polyacrylic acid doped with metal oxides have been used for dye degradation with antimicrobial properties [7]. More than 99 % of color degradation has been reported from these compounds. Some of these copolymers also show good synergistic microbicidal and catalytic effects, too [8].

Cs graft copolymers have also been developed with conducting polymers for a long time, and these polymers have found new applications in conducting, sensing properties, and medicine [3,9,10]. Grafting the next polymer to chitosan happens by oxidizing amino groups and creating active centers, which lead to the creation of nucleation centers for the growth of the next grafted polymer. This process is done both chemically and electrochemically. The prepared homopolymers are easily removed from the environment by acid washing. Poly para or ortho–toluidine (POT) is like polyaniline (PANI) but has better solubility and processability. However, it has less electrical conductivity than polyaniline. Therefore, the polymer has more functional aspects than other conductive polymers [11]. On the other hand, the grafting of PANI and POT to chitosan was prepared by chemically and electrochemically methods [12,13]. In the previous work, we prepared an aniline copolymer graft on chitosan chemically and electrochemically, and then carefully examined the kinetics of this reaction [12,14]. In the current research work, ortho-toluidine monomer is grown on chitosan and a suitable copolymer bond with electrical conduction properties is created. This property increases the antibacterial ability of the polymer. Therefore, the grafting of ortho-toluidine onto chitosan was carried out by chemically and electrochemically polymerization. Cs-*g*-POT shows a modification of ortho-toluidine such as solubility, flexibility, and film formation. In addition, due to the presence of methyl groups and more electron flow on the polymer surface, we expect to have more antibacterial properties from this copolymer than chitosan and polyaniline copolymer [15]. In the following, the grafting percentage and efficiency as well as the electrical conductivity of the obtained copolymer were measured with high accuracy. Fig. 1 shows an illustration of the chemical formation of Cs-*g*-POT.
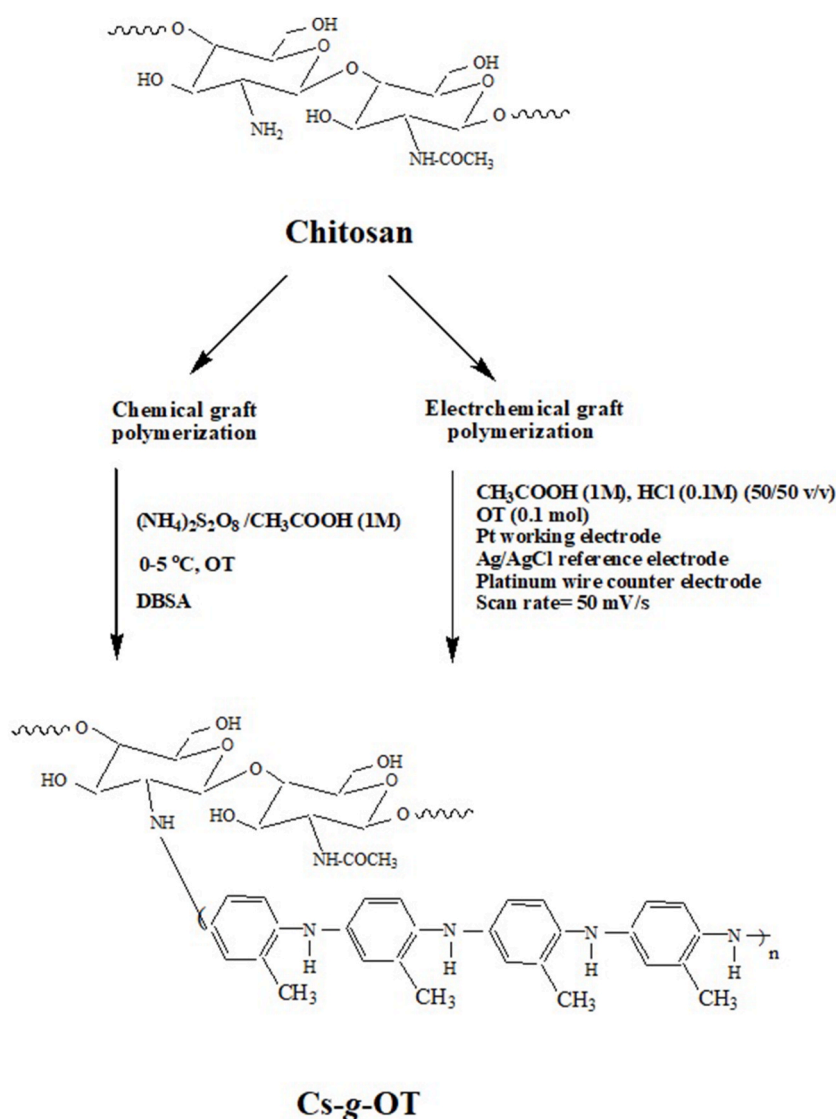

Fig. 1. Schematic illustration of chemical formation of Cs-*g*-POT.

2. Experimental

2.1. Materials

The pure chitosan was purchased from Fluka Chemical Co. The relevant degree of deacetylation was greater than 87 % and the MW was about 600,000. According to the references, chitosan powders was dried under vacuum at room temperature. Ortho-toluidine (OT) has been obtained from Merck and purified by distillation in a vacuum. Ammonia persulfate (APS), dodecyl benzene sulfonic acid (DBSA), and other chemicals were purchased from Merck Chemical Company. Here, standard control bacterial strains were used, which have appropriate antibiotic sensitivity. These strains were obtained from a reliable source such as the American Type Culture Collection (ATCC). The control strains used in this research included *E. coli* ATCC 25922, *P. aeruginosa* ATCC 27853, and *S. aureus* ATCC 25923, which were purchased from the National Center for Genetic and Biological Resources of Iran.

2.2. Characterizations

Electrical conductivity of samples were investigated with a four-probe method (homemade, according to ASTM Standards, F 43–93). Electrochemical polymerization was carried out using digital potentiate (METROHM 746 VA) by cyclic voltammetry. FTIR measurement, (Bruker) was used in spectral measurements of the polymer and graft copolymer with KBr disk. Accordingly, sharp, weak, medium, and broad peaks. FT-^{1}H NMR spectra were recorded at 250 MHz on a Bruker WP 200 SY spectrometer. NMR data is reported in the following order in d^6-DMSO as solvent: chemical shift (ppm), spin multiplicity (as singlet, doublet, triplet, quartet, multiple, and broad peaks), and integration. UV–visible spectrum was obtained by PerkinElmer Lambda 15 Spectrophotometer with N-methyl pyrrolidon solvent. Thermal analysis of the polymer was performed by Thermogravimetric Analysis (TGA) and Differential Scanning Calorimetry (DSC) using TGA-PL and DSC-Maia-200 F3 devices respectively. The study of polymer surface morphology type proceeded by Scanning Electron Microscopy (SEM) technique employing VEGA II TESCAN SEM.

2.3. Chemical synthesis of chitosan/poly ortho-toluidine graft copolymer (Cs-g-POT)

In a 250 mL container with four openings equipped with gas inlet and outlet, condenser, stirrer and thermometer, 0.1 g of high molecular weight chitosan is placed along with 40 mL of 2 % acetic acid and stirred well until it is completely dissolved under argon atmosphere and degassed. A solution of 0.448 g (0.002 mol) APS in 20 mL 2 % acetic acid was added to the chitosan solution. The mixture was kept under Ar atmosphere and at 0-4 °C. Then 0.250 g (0.0023 mol) ortho-toluidine (OT) and 0.15 g DBSA were suspended in 10 mL distilled water and was added dropwise to the above solution via a syringe through a rubber septum. The solution was reacted at 0-4 °C temperature with magnetic stirring in Ar atmosphere for 4 h. The dark green precipitate was filtrated and washed with distilled water, acetone HCl (1 M), and diluted formic acid. Dried at 60 °C for 12 h under vacuum, a greenish-black powder was obtained.

2.4. Electrochemical preparation of chitosan-poly ortho-toluidine graft copolymer (Cs-g-POT)

Firstly, a thin film of chitosan is formed on the surface Pt disk working electrode by casting method. The above electrode is placed in 20 mL of an acidic solution of 50:50 (v/v) mixtures of 1 M CH$_3$COOH and 0.1 M HCl Polymerization was carried out in a standard three-electrode cell, working electrode (Pt disk), auxiliary or counter electrode (Pt wire) and reference electrode (Ag/AgCl). For 5 min, the above electrolyte solution was well stirred by argon gas and deoxygenated, and then 0.001 M OT monomer was added to it. The range of potential and scanning rate were about 0–2 V and 50 mV/s, respectively.
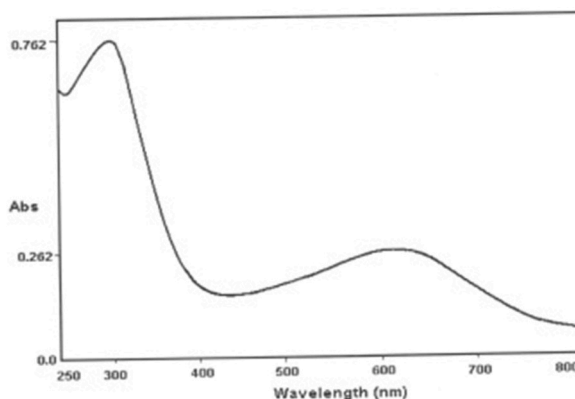

Fig. 2. UV–visible of Cs-g-POT in DMSO solvent.

3. Results and discussion

In this research work, we used chitosan as a polysaccharide with grafting, antibacterial, good processability, and high biodegradability. On the other hand, conductive polymers can be grafted on this polymer both chemically and electrochemically. This issue can help the effectiveness of chitosan's antibacterial properties and on the other hand, add new properties such as higher conductivity and strength to it and create new applications.

3.1. Study of UV–visible spectroscopy

In addition to having heteroatoms, conductive polymers have conjugated double bonds along their polymer chain, so they have electron transfers n-π^* and π-π^* which could be identified well in UV–visible and are very important characteristics of them.

Of course, the transitions π-π^* which are the result of conjugated and movable double bonds along polymer chains, are related to polaron and bi-polaron intermediate states.

Fig. 2 shows UV–visible spectrum data for Cs-*g*-POT in N-methyl pyrrolidone solvent. As we expect from a POT pattern, the first two peaks that appeared in the region of 260 and 320 nm are related to the electron transfers of n-π^* heteroatoms and π-π^* benzene rings, respectively. Due to the increase of the conjugated double bond along the length of the chain, the excited electron density has increased, and as a result, the intensity of absorption and the corresponding wavelength should increase. As the length of the polymer chain increases and because of conjugated double bonds, the electron density is increased, so the electron transfer of π-π^* transitions also increases. This issue has increased dramatically with polymer doping and with the creation of polaron and bi-polaron transition states, the intensity of absorption and the corresponding wavelength increases and finally shows itself in the region of 550–700 nm. As we know, this is one of the important characteristics of conducting polymers. These transitions are obviously related to the benzenoid diamine and quinoid diimine forms of ortho-toluidine (OT) rings.

3.2. Infrared spectroscopy

The FTIR spectroscopic characteristics of grafted polymer (Cs-*g*-POT) are shown in Fig. 3. As it is clear in the figure, this spectrum confirms the description of the polymer substructure. The strong peak observed in the region 3419 cm^{-1} is related to the O–H and N–H stretching vibrations that overlapped each other and confirms the presence of polysaccharide. In addition, the peaks related to stretching vibrations O–H and N–H of the polymer also appear in the region of 3000–3419 cm^{-1}, which overlaps with the chitosan peaks. The decrease in the intensity of peaks related to chitosan is also due to participation in the formation of copolymer. The shoulder peak observed in the region of 2919 cm^{-1} is related to the stretching vibrations of aliphatic C–H of methyl group OT and methylene groups of chitosan. The peaks at 1629 and 1514 cm^{-1} are attributed to C=N and C=C stretching modes of the POT ring (benzenoid diamine and quinoid diimine forms). The specific peak around 1259 cm^{-1} is associated with vibrational modes of N = Q = N (quinoid diimine rings), indicating that POT is formed. The wide peak at 1041 cm^{-1} is attributed to C–O and C–N stretching that so observed together. From the IR data, the Cs-*g*-POT shows specific signs for POT and Cs, which confirms the successful grafting of POT on Cs.

3.3. NMR spectroscopy

Fig. 4 shows the FT-^{1}H NMR of grafted polymer chit-*g*-POT. The wide signs shown in areas 1.9–2.2 ppm represent the different protons of CH$_3$ and CH$_2$ in the chitosan and grafted chains. On the other hand, the high mark marked in area 2.4 ppm is indicates the C–H protons of Cs, which overlap with the protons of the solvent. The peak in region 3.3 ppm corresponds to the protons of the hydroxyl group of Cs, which is slightly longer due to the overlap with water protons. Finally, the wide peaks in the 6.8–7.5 ppm region
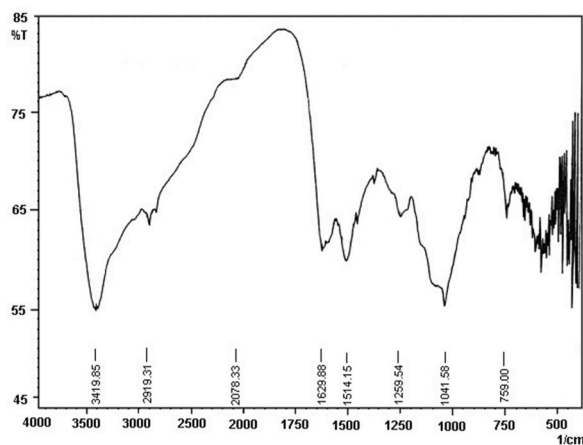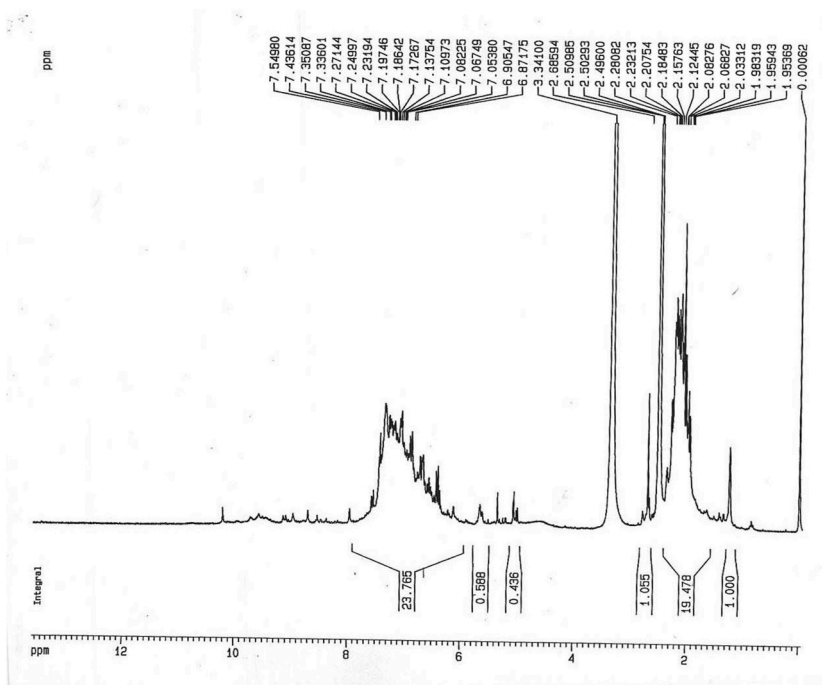

Fig. 3. FTIR spectrum of Cs-*g*-POT.

Fig. 4. FT-1H NMR spectrum of Cs-*g*-POT.

are related to CH-aromatic in POT.

3.4. Study of DSC and TGA graphs

Fig. 5 shows STA (DSC and TGA) thermograms of chitosan and Figs. 6 and 7 show TGA and DSC thermograms of Cs-*g*-POT respectively. The graphs show that the copolymer has a higher thermal resistance than Cs, but it is still lower than POT. Graph TGA related to Cs shows that this polymer starts to soften at a temperature between 200 and 210 °C. In the DSC curve for chitosan, one
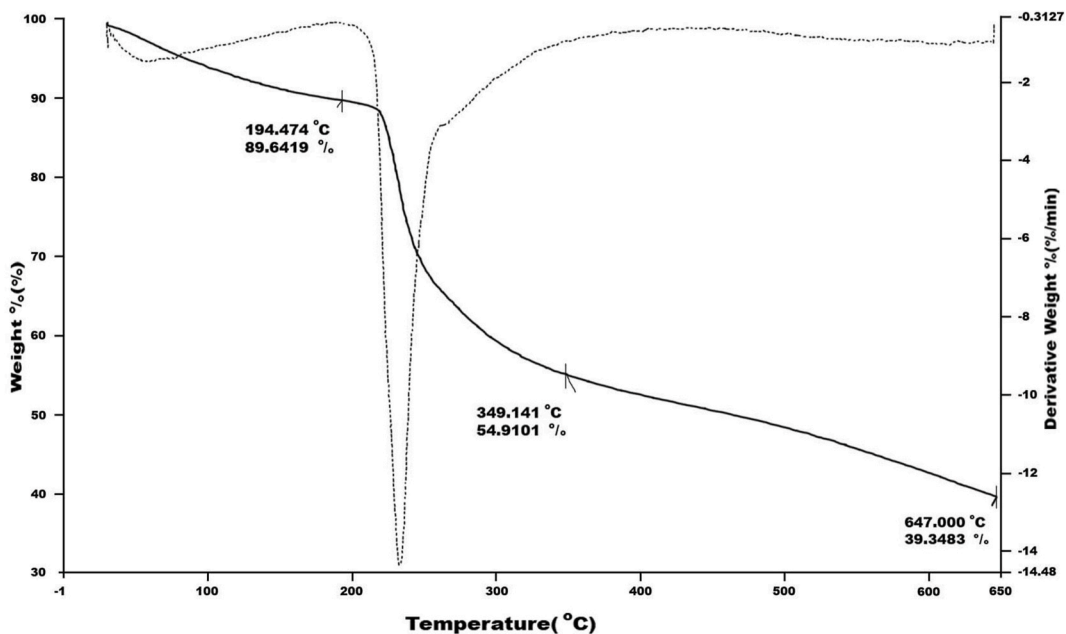

Fig. 5. STA (TGA and DSC) thermograms of chitosan.

endothermic peak appeared in the 230 °C region and degradation initiation was showed in higher than 230 °C. TGA thermogram of Cs-*g*-POT showed that the polymer started to soften at 50 °C and up to 120 °C it lost approximately 7.3 % of its weight which is due to the removal of residual moisture and solvent in the copolymer. Cs-*g*-POT shows thermal stability below 170 °C. At above 220 °C polymer starts to degrade and complete degradation occurs at 530 °C. The TGA results for Cs-*g*-POT with 25 % grafted POT illustrate that initial decomposition temperature (IDT), copolymer decomposition temperature (PDT) and the maximum copolymer decomposition temperature (PDTmax) are 170 °C, 250 °C and 515.68 °C respectively. The residual weight (γc) of the Cs-*g*-POT was reported at 612.53 °C to be 53.629 %. Fig. 7 shows the DSC analysis of the Cs-*g*-POT. As it is clear from the curve, this copolymer has three endothermic ranges at 98.3, 221.6, and 267.6 °C. This can be related to the energy absorbed in the three stages of separating the grafted polymer, breaking the biopolymer, and breaking down poly ortho–toluidine. These thermal behaviors are fully consistent with the thermal decomposition analysis of TGA.

3.5. Scanning electronic microscopy

Fig. 8a and b shows surface and cross-section SEM images for Cs-*g*-POT. The remarkable growth of the chain and high degree of grafting are evident from the images. Fig. 8a clearly depicts the morphology of the two polymers i.e., Cs (upper layer) and grafted POT (lower layer). It is clear from SEM images that the co-polymer to some extent shows hydrogel properties. The voids on the surface and local swellings in the bulk of co-polymer are addressed to hydrogel properties.

3.6. Study of cyclic voltammetry

The cyclic voltammograms for Cs-*g*-POT film grown and blank at 50 mV/s scan rate in acidic solution, Pt disk as working electrode, Pt wire as a counter electrode, and Ag/AgCl as reference electrode, with a reduced anodic potential limit, are shown in Fig. 9a,b.

First, a thin film of Cs was coated on the surface of the working electrode, and then, by creating a suitable potential and scan rate, in the presence of OT (0.001 mol) monomer and in an acidic conditions, the Cs-*g*-POT film Cs-*g*-POT film was prepared on the surface of the platinum electrode. The electrolyte solution used was 20 mL of 50:50 (v/v) mixtures of 1 M acetic acid and 0.1 M HCl in water. The potential range for electrochemical polymerization and the scan rate were about 0–2 V (versus Ag/AgCl) and 50 mV/s, respectively.

3.7. Efficiency and grafting percentage measurements

Determining the grafting percentage and efficiency has an important role in grafting copolymer applications. The amount of these two items depends on the monomer concentration, kind of initiator, reaction time, and temperature. There are different methods to control the grafting percentage and efficiency, and here the gravimetric method was used. They can control the final properties of the copolymer [16,17].

The weight of chitosan used is W_1 (g) and the weight of graft copolymer and homopolymers is considered W_2 (g). On the other hand, with continuous extraction with a suitable solvent, the homopolymer is separated from the reaction medium and the copolymer. Then the resulting final polymer was washed with ice methanol and dried slowly under a vacuum, and it was called W_3 (g)(Cs-*g*-POT). The difference in (W_3–W_1) gives the weight of the grafted polymer (POT). The difference in (W_2–W_3) gives the weight of the homopolymer POT and the weight of the polymer grafted and homopolymer gives W_4 (g). Therefore, according to the above references and materials, the following calculations can be performed to measure the grafting percentage and the production efficiency of the copolymer.

$$W_1 = 0.20, W_3 = 0.34, W_4 = 0.36$$

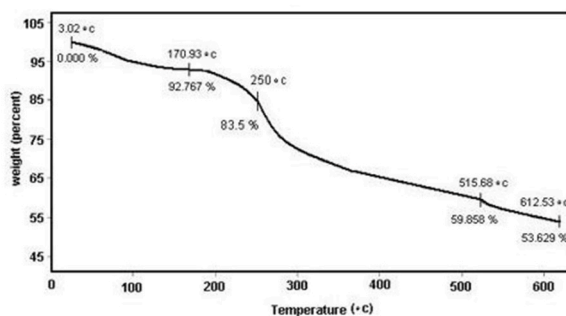$$Grafting\ \% = \frac{weight\ of\ Cs-g-POT}{weight\ of\ Cs} \times 100$$
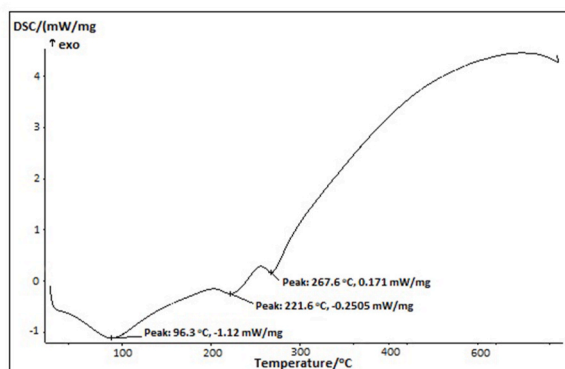

Fig. 6. TGA thermograms of Cs-*g*-POT.

Fig. 7. DSC thermograms of Cs-*g*-POT.

$$Grafting\ \% = \frac{W_3 - W_1}{W_1} \times 100$$

$$Grafting\ \% = \frac{0.34 - 0.20}{0.20} \times 100 = 70.00$$

$$Efficiency\ \% = \frac{weight\ of\ Cs - g - POT}{weight\ of\ polymer\ grafted\ and\ homopolymer} \times 100$$

$$Efficiency\ \% = \frac{W_3 - W_1}{W_4} \times 100$$

$$Efficiency\ \% = \frac{0.34 - 0.20}{0.36} \times 100 = 38.88$$

3.8. Studying antibacterial property of copolymer by disc diffusion method

Here, the effect of Cs-*g*-POT was studied using the disk diffusion method. The method was adopted by Jiang et al. with some modifications [18]. Briefly, Mueller-Hinton agar plates were prepared and inoculated with three different bacteria, *Escherichia coli* (*E. coli*) and *Pseudomonas aeruginosa* (*P. aeruginosa*) as Gram-negative bacteria, and *Staphylococcus aureus* (*S. aureus*), as Gram-positive bacterium with about 1×10^5 CFU/plate. Then, 50 μg of the compound was loaded on a round-shaped paper with 10 mm diameter and placed on plates. The plates were incubated at 37 °C for an overnight. The antibacterial activity of the copolymer was estimated using the measurement of the diameter of the inhibition zone. To compare the antibacterial activity of the compounds, tetracycline antibiotic with a concentration of 50 μg per disk was used as a positive control and sterilized PBS buffer was used as a negative control. Cs-*g*-POT had an inhibitory effect on three bacteria; while the negative control had no effect on the bacterial growth (no inhibition zone was observed), the diameter of the inhibition zone around the Cs-g-POT on *E. coli*, *P. aeruginosa,* and *S. aureus* plates were 15, 13 and 11 mm, respectively. As was expected, tetracycline has also an inhibitory effect on all bacteria (the inhibition zone on *E. coli*, *P. aeruginosa,* and *S. aureus* plates were 25, 24, and 23 mm, respectively).

3.9. Studying antibacterial property of copolymer by minimum inhibitory concentration (MIC)

To determine the minimum inhibitory concentration (MIC) of Cs-*g*-POT, the MIC method was exploited. For this aim, 100 μL of the bacterial cultures containing 1×10^6 colony-forming units (CFU) was added to a 96-well plate. Then, different concentrations of the copolymer (1, 5, 10, 20, 40, and 80 μg/mL) were added to each well and the plate was incubated at 37 °C for overnight. 50 μL of the supernatant was taken out and the optical density (OD) of the media was read at a wavelength of 600 nm using a spectrophotometer. Using Equation (1), the inhibition activity (I %) was calculated.

$$I\ (\%) = (OD_{control} - OD_{sample})/OD_{control} \times 100\% \tag{1}$$

where OD_{sample} and $OD_{control}$ are OD values at 600 nm of the bacterial supernatant without any treatment and the bacterial supernatant with treatment with different samples, respectively [19]. Fig. 10 shows the antibacterial activity of different concentrations of the Cs-*g*-POT on three different bacteria, *E. coli*, *P. aeruginosa,* and *S. aureus, respectively*. To obtain the inhibition activity (I), the OD of the culture media was measured at 600 nm and I (%) was calculated according to Equation (1). Statistical analysis using Graph Pad Prism software showed that the copolymer has an inhibitory effect on the growth of tested bacteria, *E. coli*, *P. aeruginosa,* and *S. aureus*. In all tested concentrations the copolymer could inhibit the growth of *E. coli* and *P. aeruginosa,* significantly. According to Fig. 10, the
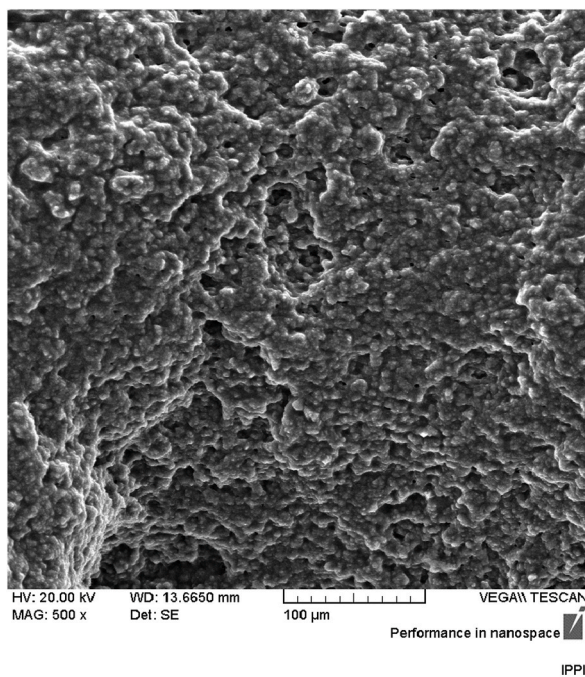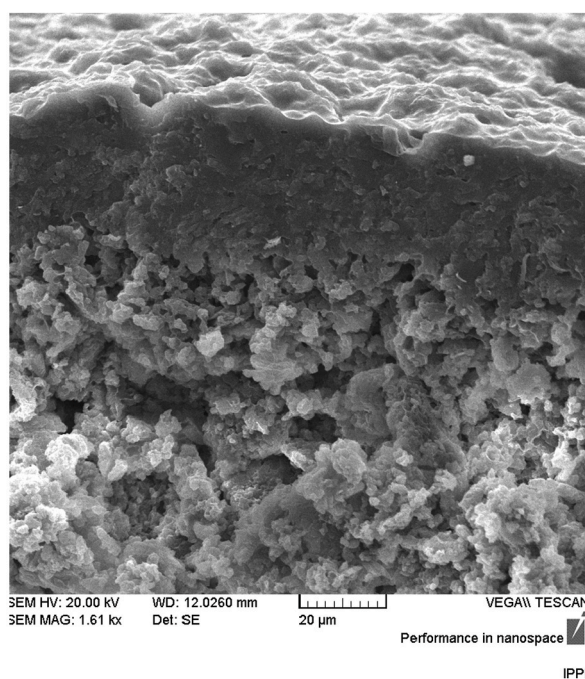
Fig. 8. SEM micrographs of Cs-*g*-POT, (a) surface image, and (b) cross-section image of Cs-*g*-POT.

copolymer shows a very good inhibitory effect against all three bacteria and these effects start from under 1 μg. However, the inhibitory properties of gram-negative bacteria are more than gram-positive, and in the meantime, *E. coli* shows the best inhibitory effect rather than *S. aureus*. The obtained results from two exploited methods, disk-diffusion, and MIC, were compatible. Cs-*g*-POT had a more inhibitory effect on *E. coli* rather than *P. aeruginosa* and *S. aureus*.
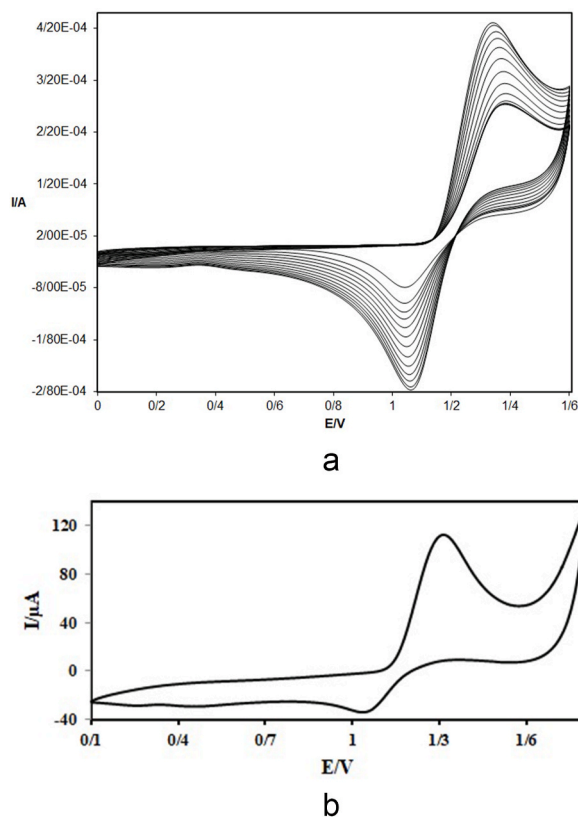
Fig. 9. Cyclic voltammograms of a) graft copolymer formation of Cs-*g*-POT and b) blank of Cs-*g*-POT at 50 mV/s scan rates, in aqueous 1 M acetic acid, 0.1 M HCl (50/50 v/v) solution, Pt disk electrode, platinum wire counter electrode and Ag/AgCl reference electrode.
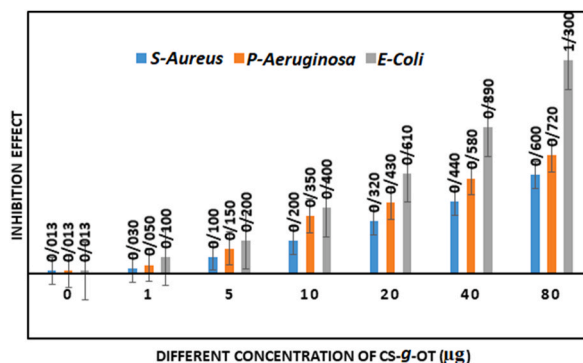

Fig. 10. Inhibition activity of the Cs-*g*-POT on *E. coli*, *P. aeruginosa* and *S. aureus*.

3.10. Antibacterial properties of Cs-g-POT

The antibacterial property of chitosan is due to the high density of amine groups on the surface of the polymer, which becomes cationic in acidic environments. As a result, the positively charged surface due to the oxidation of amino groups in chitosan affects the attached bacteria and causes osmotic imbalance and stimulation of peptidoglycan layer hydrolysis and leakage of intracellular electrolytes and finally the death of bacteria. In addition to these properties, POT has the ability to deal with all kinds of bacteria by transferring electrons and Schweitzer ion (dopant, pseudo-surfactant). Fig. 11 schematically shows that the formation of free radicals and electrons from the conducting copolymer can easily penetrate into the cell wall by destroying it and accelerate cell death by oxidative (ROS) destruction. Cs-*g*-POT has a movable positive charge due to the presence of a dopant, and the corresponding Schweitzer ion is also a moving negative ion. In this way, the bacteria are slowly attracted to the polymer surface and start polar-polar interactions with each other. In addition to these ionic interactions, due to the electron motion of the copolymer, electron transfers also
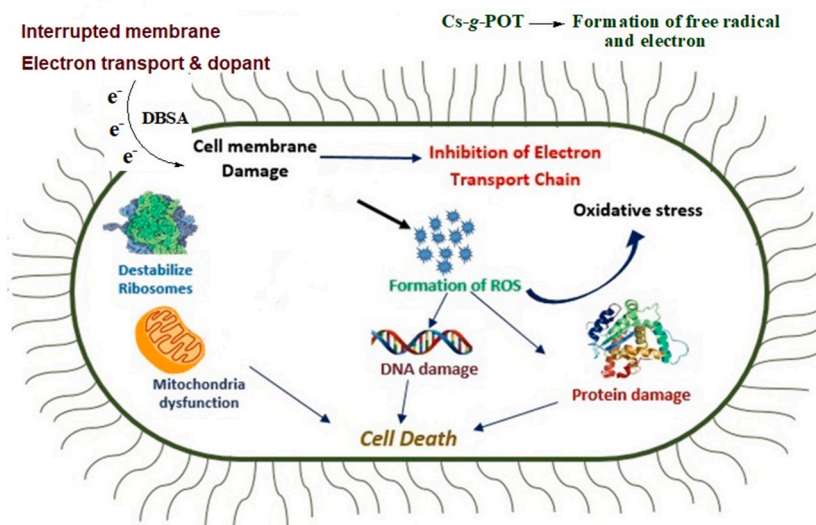
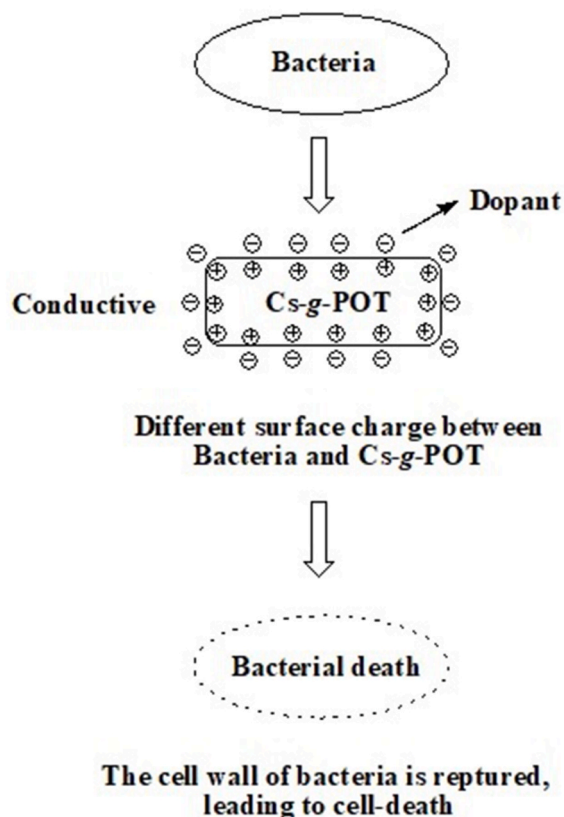**Fig. 11.** Destruction of the bacterial cell membrane by Cs-*g*-POT.

Fig. 12. The general outline of the antibacterial mechanism of Cs-g-POT.

occur on the surface. The general outline of the antibacterial mechanism of Cs-g-POT is shown in Fig. 12, where the active center is produced, and the semi-surfactant part is specified. Both factors destroy the liposaccharide wall of the bacteria, and the death of the bacteria begins.

4. Conclusion

The resulting homogeneous Cs-g-POT co-polymer simultaneously shows suitable solubility with high physical stability and excellent processability properties. The antibacterial property of the copolymer was studied on *E. coli*, *P. aeruginosa,* and *S. aureus* as gram-negative and positive bacteria as common bacterium in skin wounds. It has a unique ability to destroy the cell wall of both types of bacteria and it is more effective than gram-negative bacteria. The obtained results from the two exploited methods were compatible. It was fully eradicated after 15 min of exposure. Bacteria are adsorbed on the surface of the polymer by polar-polar and Van Der Waals interactions, where they undergo cell lysis by dopant and electron transfer, and eventually bacterial cell death. The time of effect and destruction of the bacterial wall is much faster than other polymers for the reasons mentioned (From a few seconds to a minute). It seems that these types of polymers are good candidates for anti-fungal and anti-virus polymers. As it is clear from the results, POT has more solubility and better antibacterial properties than the latest research done in this field (chitosan and polyaniline graft copolymer [15]).

Availability of data and materials

Data associated with the study has not been deposited into a publicly available repository. Data are available from the corresponding author upon reasonable request.

Data and code availability

Not Applicable.

Ethical approval

Not Applicable.

CRediT authorship contribution statement

Sama Sadat Hosseini: Methodology. **Seyed Hossein Hosseini:** Writing – original draft, Methodology, Data curation, Conceptualization. **Abbas Hajizade:** Formal analysis.

Declaration of competing interest

The authors declare the following financial interests/personal relationships which may be considered as potential competing interests: Seyed Hossein Hosseini reports was provided by Nika Pooyesh Industrial Research Institute. Seyed Hossein Hosseini reports a relationship with I am CEO of Nika Pooyesh Industrial Research Institute that includes: board membership and employment. Sama Sadat Hosseini has patent pending to NP Institute. Author 1: Sama Sadat Hosseini, conducting a research and investigation process, specifically performing the experiments, or data/evidence collection. Author 2: Seyed Hossein Hosseini, corresponding and Ideas; formulation or evolution of overarching research goals and aims. Author 3: All antibacterial experiments.

The authors declare no conflicts of interest and all of them are working only in the institute.

If there are other authors, they declare that they have no known competing financial interests or personal relationships that could have appeared to influence the work reported in this paper.

Acknowledgments

We acknowledge financial and laboratory support from the Nika Pooyesh Industrial Research Institute.

References

[1] J. Yu, D. Wang, N. Geetha, K.M. Khawar, S. Jogaiah, M. Mujtaba, Current trends and challenges in the synthesis and applications of chitosan-based nanocomposites for plants: a review, Carbohydr. Polym. 261 (2021) 117904. http://doi:10.1016/j.carbpol.2021.117904.
[2] S.M.A. Soliman, M.F. Sanad, A.E. Shalan, Synthesis, characterization and antimicrobial activity applications of grafted copolymer alginate-g-poly (N-vinyl imidazole), RSC Adv. 11 (2021) 11541–11548. http://doi:10.1039/d1ra01874d.
[3] D. Kumar, S. Gihar, M.K. Shrivash, P. Kumar, P.P. Kundu, A review on the synthesis of graft copolymers of chitosan and their potential applications, Int. J. Biol. Macromol. 163 (2020) 2097–2112. http://doi:10.1016/j.ijbiomac.2020.09.060.
[4] T.M. Tamer, E.R. Kenawy, M.M. Agwa, S.A. Sabra, M.A. El-meligy, M.S. Mohy-Eldin, Wound dressing membranes based on immobilized Anisaldehyde onto (chitosan-GA-gelatin) copolymer: in-vitro and in-vivo evaluations, Int. J. Biol. Macromol. 211 (2022) 94–106. http://doi:10.1016/j.ijbiomac.2022.05.061.
[5] Z.D. Yu, M.K. Hyun, J.C. Hyoung, Conducting polymer-based electro-responsive smart suspensions, Chem. Pap. 75 (2021) 5009–5034. http://doi:10.1007/s11696-021-01550-w.

[6] S.H. Hosseini, M. Tarakameh, S.H. Hosseini, Preparation of thermal neutron absorber based B4C/TiO2/polyaniline nanocomposite, Int. J. Phys. Sci. 15 (2020) 49–59. http://doi:10.5897/ijps2019.4851.

[7] Muhammad Waqas, Anum Shahzadi, Haider Ali, Anwar Ul Hamid, Mohammed M. Algaradah, Hisham S.M. Abd-Rabboh, Muhammad Ikram, Chitosan grafted polyacrylic acid doped MnO_2 nanocomposite an efficient dye degrader and antimicrobial agent, Int. J. Biol. Macromol. 251 (2023) 126343, https://doi.org/10.1016/j.ijbiomac.2023.12634.

[8] Ehtisham Umar, Haider Ali, Iram Shahzadi, Anwar Ul Hamid, Hameed Ullah, Sherdil Khan, Muhammad Ikram, In-vitro synergistic microbicidal and catalytic evaluation of polyvinylpyrrolidone/chitosan doped tungsten trioxide nanoplates with evidential in-silico analysis, Int. J. Biol. Macromol. 242 (2) (2023) 124815, https://doi.org/10.1016/j.ijbiomac.2023.124815.

[9] M. Kaliva, A. Georgopoulou, D.A. Dragatogiannis, C.A. Charitidis, M. Chatzinikolaidou, M. Vamvakaki, Biodegradable chitosan-graft-poly (l-lactide) copolymers for bone tissue engineering, Polymers 12 (2020) 316, https://doi.org/10.3390/polym12020316.

[10] G. Alberti, C. Zanoni, V. Losi, L.R. Magnaghi, R. Biesuz, Current trends in polymer based sensors, Chemosensors 9 (2021) 108, https://doi.org/10.3390/chemosensors9050108.

[11] M.S. Zoromba, M.H. Abdel-Aziz, M. Bassyouni, A. Attar, A.F. Al-Hossainy, Synthesis and characterization of Poly (ortho-aminophenol-co-para-toluidine) and its application as semiconductor thin film, J. Mol. Struct. 1225 (2021) 129131. http://doi:10.1016/j.molstruc.2020.129131.

[12] S.H. Hosseini, J. Simiari, B. Farhadpour, Chemical and electrochemical grafting of polyaniline onto chitosan, Iran. Polym. J. (Engl. Ed.) 18 (2009) 3–13.

[13] D.F. Katowah, M.M. Rahman, M.A. Hussein, T.R. Sobahi, M.A. Gabal, M.M. Alam, A.M. Asiri, Ternary nanocomposite based poly(pyrrole-co-O-toluidine), cobalt ferrite and decorated chitosan as a selective Co2+ cationic sensor, Compos. B Eng. 175 (2019) 107175. http://doi:10.1016/j.compositesb.2019.107175.

[14] S.H. Hosseini, Ammonium persulphate initiated graft copolymerization of aniline onto chitosan-A comparative kinetic study, International Journal of Advanced Science and Engineering 7 (2021) 1975–1982. http://doi:10.29294/ijase.7.4.2021.1975-1982.

[15] S.S. Hosseini, A.R. Jahandideh, S.P. Mortazavi, S.H. Hosseini, Evaluation of antimicrobial activity of chitosan and polyaniline nanocluster graft copolymer, Polym. Bull. (2024). In Press-2024.

[16] I.S. Sani, M. Rezaei, A.B. Khoshfetrat, D. Razzaghi, Preparation and characterization of polycaprolactone/chitosan-g-polycaprolactone/hydroxyapatite electrospun nanocomposite scaffolds for bone tissue engineering, Int. J. Biol. Macromol. 182 (2021) 1638–1649. http://doi:10.1016/j.ijbiomac.2021.05.163.

[17] M.Á. Vega-hernández, G.S. Cano-díaz, E. Vivaldo-lima, A. Rosas-aburto, M.G. Hernández-luna, A. Martinez, J. Palacios-alquisira, Y. Mohammadi, A. Penlidis, A review on the synthesis, characterization and modeling of polymer grafting, Processes 9 (2021) 1–85. http://doi:10.3390/pr9020375.

[18] L. Jiang, Z. Zhu, Y. Wen, S. Ye, C. Su, R. Zhang, W. Shao, Facile construction of functionalized GO nanocomposites with enhanced antibacterial activity, Nanomaterials 9 (2019) 913. http://doi:10.3390/nano9070913.

[19] G.A. Marcelo, J. Galhano, M.P. Duarte, J.L. Capelo-Martínez, C. Lodeiro, E. Oliveira, Validation of a standard luminescence method for the fast determination of the antimicrobial activity of nanoparticles in Escherichia coli, Nanomaterials 12 (2022) 2164. http://doi:10.3390/nano12132164.